

## Interface optical phonons in $k$ -component Fibonacci dielectric multilayers

R. W. Peng, G. J. Jin, Mu Wang, A. Hu, S. S. Jiang, and D. Feng

*National Laboratory of Solid State Microstructures, Nanjing University, Nanjing 210093, China  
and Center for Advanced Studies in Science and Technology of Microstructures, Nanjing 210093, China*

(Received 15 June 1998; revised manuscript received 14 September 1998)

We present the studies of the interface optical phonons in  $k$ -component Fibonacci (KCF) dielectric multilayers, in which  $k$  different incommensurate intervals are arranged according to a substitution rule. In the dielectric continuum approximation, the dispersion relations and the frequency spectra are obtained by the transfer-matrix method. Free-boundary and periodic-boundary conditions are taken into account. With the free-boundary condition, the dispersion relations of the interface optical phonons in the KCF multilayers are demonstrated to possess two bands of dual structures. For the KCF multilayers with  $1 < k \leq 5$ , each subband is a self-similar structure and contains  $k + 1$  filial generations; for the KCF multilayers with  $k > 5$ , the sub-bands do not show self-similarity, but they still have the hierarchical characteristic (where  $k$  is the number of different incommensurate intervals). In the case of the periodic-boundary condition, the frequency span of interface optical phonons in the KCF multilayers is singularly continuous and the frequency spectra are analyzed by a multifractal concept. A dimensional spectrum of singularities associated with the frequency spectrum,  $f(\alpha)$ , demonstrates that in the KCF multilayers the interface optical phonons distribution presents a genuine multifractality. It is also shown that by increasing the number of different incommensurate intervals in KCF multilayers, the fractal dimension of the corresponding support decreases. [S0163-1829(99)06205-0]

### I. INTRODUCTION

Recently much attention has been paid to elementary excitations in artificial multilayers. The interest has been focused particularly on magnons,<sup>1</sup> plasmons,<sup>2</sup> and phonons.<sup>3</sup> In phonon studies, the optical phonon in alkali halide or polar semiconductor multilayers is rather attractive.<sup>4</sup> It is well known that there are two kinds of optical modes: bulklike excitation and interface phonons. In the multilayer systems, the excitations in individual layers are coupled each other by the tail of evanescent field.<sup>5</sup> Hence the interface phonons are coupled to induce the collective excitation of the whole multilayer system when the layer thickness is relatively thin. Since the coupling of different layers depends critically upon the structure of multilayers, it is interesting to investigate the interface optical phonons in the dielectric multilayers with various configurations, such as periodic, quasiperiodic and even other aperiodic structures.

The Fibonacci sequence is one of the well-known examples in one-dimensional (1D) quasiperiodic structures. The Fibonacci sequence can be produced by repeated application of the substitution rule  $A \rightarrow AB$  and  $B \rightarrow A$ , in which the ratio of the numbers of the two incommensurate intervals  $A$  and  $B$  is equal to the golden mean  $\tau = (\sqrt{5} + 1)/2$ . Since the first realization of Fibonacci superlattices reported by Merlin *et al.*,<sup>6</sup> a lot of works on physical properties of 1D quasiperiodic structures have been carried out both experimentally and theoretically.<sup>7</sup> For example, the exotic wave phenomena of Fibonacci systems in x-ray scattering spectra,<sup>8</sup> Raman scattering spectra,<sup>9</sup> and in propagation modes of acoustic waves on corrugated surfaces<sup>10</sup> have been investigated. However, only a few studies of optical interface modes in Fibonacci dielectric superlattices have been reported,<sup>4,11</sup> and to our knowledge, there seems no work on the interface optical phonons in 1D aperiodic structures with more than two

incommensurate intervals, although their structural characterization and other physical properties have been investigated previously.<sup>12,13</sup>

In this paper, we investigate the interface optical phonons in  $k$ -component Fibonacci (KCF) dielectric multilayers, which contain  $k$  incommensurate intervals  $A_i$  ( $i = 1, 2, \dots, k$ ) and can be generated by the substitute rule  $A_1 \rightarrow A_1 A_k$ ,  $A_k \rightarrow A_{k-1}, \dots, A_i \rightarrow A_{i-1}, \dots, A_2 \rightarrow A_1$ . In the dielectric continuum approximation, the dispersion relation and frequency spectra are achieved by a transfer-matrix method. We discuss the interface optical phonons in the KCF dielectric multilayers with free-boundary condition and periodic-boundary condition, respectively. It is shown that with free boundary condition, the dispersion relations of interface optical phonons possess two dual bands. For the KCF multilayers with  $1 < k \leq 5$ , which are quasiperiodic, each subband is a self-similar structure with  $k + 1$  filial generations; while for the KCF multilayers with  $k > 5$ , which are nonquasiperiodic, the sub-bands only show the hierarchical characteristic. On the other hand, with periodic boundary condition, the frequency distribution for the KCF dielectric multilayer is singularly continuous and multifractal analysis is employed to characterize these frequency spectra. It is known that multifractal analysis is a suitable statistical description for the study of long term dynamical behavior of a physical system.<sup>14,15</sup> Our investigation demonstrates that the frequency distribution of interface optical phonons in the KCF multilayers present scaling properties of multifractal indeed.

### II. THE THEORETICAL MODEL

To begin with, we give a description of the  $k$ -component Fibonacci structures (KCFS). We define a basis which includes  $k$  distinct incommensurate intervals  $A_1, A_2, \dots, A_k$ . These intervals are arranged in a  $k$ -component Fibonacci se-

quence with a substitution rule  $S$  denoted as

$$S \left\{ \begin{array}{l} A_1 \rightarrow A_1 A_k, \\ A_k \rightarrow A_{k-1}, \\ \dots, \\ A_i \rightarrow A_{i-1}, \\ \dots, \\ A_2 \rightarrow A_1. \end{array} \right.$$

On the other hand, the KCFS can also be expressed as the limit of the generation of the sequence,  $C_n^{(k)}$ . Let  $C_n^{(k)} = S^n A_1$ , it follows  $C_0^{(k)} = A_1$ ,  $C_1^{(k)} = A_1 A_k$ ,  $C_2^{(k)} = A_1 A_k A_{k-1}, \dots, C_{k-1}^{(k)} = A_1 A_k A_{k-1} \dots A_3 A_2$ , and in general,  $C_n^{(k)} = C_{n-1}^{(k)} + C_{n-k}^{(k)}$ . If the interval number of the generation  $C_n^{(k)}$  is defined as  $F_n^{(k)}$ ,  $F_n^{(k)}$  is satisfied by  $F_n^{(k)} = F_{n-1}^{(k)} + F_{n-k}^{(k)}$  with  $F_i = i + 1$  ( $i = 0, 1, \dots, k-1$ ). We denote the number of  $A_i$  ( $i = 1, 2, \dots, k$ ) in  $C_n^{(k)}$  as  $N_n^{(k)}(A_i)$ . The ratios of these numbers are defined as  $\eta_i = \lim_{n \rightarrow \infty} [N_n^{(k)}(A_i) / N_n^{(k)}(A_1)]$ . It turns out that the set  $\{\eta_i\}$  satisfies

$$\eta_k^k + \eta_k = 1,$$

$$1 : \eta_k = \eta_k : \eta_{k-1} = \dots = \eta_i : \eta_{i-1} = \dots = \eta_3 : \eta_2. \quad (1)$$

Therefore all these ratios  $\eta_i = \eta_k^{k-i+1}$  ( $1 < i \leq k$ ) are irrational numbers between zero and unity except  $\eta_1 = 1$ . It has been proved<sup>12</sup> that the KCFS are quasiperiodic for  $1 < k \leq 5$ ; while for  $k > 5$ , the KCFS are nonquasiperiodic, yet they are still ordering.

The  $k$ -component Fibonacci (KCF) multilayers we studied here consist of  $k$  different kinds of layers  $A_1, A_2, \dots, A_i, \dots, A_k$  with dielectric constants  $\{\varepsilon_i(\varpi)\}$  and thicknesses  $\{d_i\}$ , respectively (where  $i = 1, 2, \dots, k$ ). Now we consider collective excitation in the KCF dielectric multilayers. In the electrostatic limit, the electrostatic potential  $\Phi$  obeys the Laplacian equation  $\nabla^2 \Phi(\mathbf{r}, t) = 0$ . Let  $z$  axis be perpendicular to the multilayer planes, we assume each layer is isotropic, so that without loss generality, the wave vector  $q$  may be taken parallel to the  $x$  axis. It follows that the electrostatic potential  $\Phi(\mathbf{r}, t)$  can be written as  $\Phi(\mathbf{r}, t) = \varphi(z) \exp\{i(qx - \varpi t)\}$ , and

$$\left( \frac{d^2}{dz^2} - q^2 \right) \varphi(z) = 0. \quad (2)$$

It is clear that the general solution of Eq. (2) can be expressed as  $\varphi_l(z) = g_l e^{qz} + h_l e^{-qz}$  in each layer, where  $l$  is an index of the layer  $A_l$ . While at the interface of layers  $A_l$  and  $A_{l+1}$ , the electrostatic continuum conditions require

$$\begin{aligned} \varphi_l(z) &= \varphi_{l+1}(z), \\ \varepsilon_l \frac{d\varphi_l(z)}{dz} &= \varepsilon_{l+1} \frac{d\varphi_{l+1}(z)}{dz}. \end{aligned} \quad (3)$$

If a local coordinate is chosen for each layer and its origin is positioned at the center of this layer, the electrostatic potential can be expressed in a matrix form as

$$\begin{pmatrix} g_{l+1} \\ h_{l+1} \end{pmatrix} = T_{l+1,l} \begin{pmatrix} g_l \\ h_l \end{pmatrix}. \quad (4)$$

The transfer matrix has the form of

$$T_{l+1,l} = \begin{pmatrix} \alpha e^{q(d_l + d_{l+1})/2} & \beta e^{q(d_{l+1} - d_l)/2} \\ \beta e^{q(d_l - d_{l+1})/2} & \alpha e^{-q(d_l + d_{l+1})/2} \end{pmatrix}, \quad (5)$$

in which  $\alpha = \frac{1}{2}(1 + \varepsilon_l / \varepsilon_{l+1})$ ,  $\beta = \frac{1}{2}[1 - \varepsilon_l / (\varepsilon_{l+1})]$ , and  $\varepsilon_l$  is the dielectric constant and  $d_l$  is the thickness of the layer  $A_l$  (where  $l = 1, 2, \dots, k$ ). In this way, the electrostatic behavior in layered medium can be achieved by multiplying matrices of the different layers.

Here we aim to study the  $k$ -component Fibonacci multilayer  $C_n^{(k)}$  sandwiched between two media of material  $A_1$ , the corresponding transfer matrix is

$$M_n^{(k)} = M_{n-k}^{(k)} M_{n-1}^{(k)}, \quad (6)$$

where  $M_0^{(k)} = T_1^{(k)}$ ,  $M_1^{(k)} = T_{k,1}^{(k)} T_1^{(k)}$ ,  $M_2^{(k)} = T_{k-1,k}^{(k)} T_{k,1}^{(k)} T_1^{(k)}$ ,  $\dots$ ,  $M_{k-1}^{(k)} = T_{2,3}^{(k)} T_{3,4}^{(k)} \dots T_{k-1,k}^{(k)} T_{k,1}^{(k)} T_1^{(k)}$ . Therefore the whole multilayer is represented by a product matrix  $M_n^{(k)}$  relating to the initial and the final electrostatic potential through the multilayer. By considering the boundary condition, the dispersion equation can be obtained. From the dispersion equation, the features of the interface optical phonons in the KCF dielectric multilayers can be derived. In the following sections, we are going to perform the calculations with two kinds of boundary conditions: the free-boundary condition and the periodic-boundary condition, respectively.

### III. DISPERSION RELATION WITH FREE-BOUNDARY CONDITION

Suppose the environment of dielectric constant is  $\varepsilon_e$ . The electrostatic potential on the left and right boundaries,  $\Phi_L$  and  $\Phi_R$ , can be written as  $\Phi_{L(R)} = \varphi_{L(R)} \exp\{i(qx - \varpi t)\}$ . The constraint equations are given<sup>4</sup> by

$$\begin{aligned} \varepsilon_1 e^{-q d_1/2} g_1 - \varepsilon_1 e^{q d_1/2} h_1 &= \varepsilon_e e^{-q d_1/2} g_1 + \varepsilon_e e^{q d_1/2} h_1, \\ \varepsilon_1 e^{q d_1/2} g_{N+1} - \varepsilon_1 e^{-q d_1/2} h_{N+1} &= \varepsilon_e e^{q d_1/2} g_{N+1} \\ &+ \varepsilon_e e^{-q d_1/2} h_{N+1}, \end{aligned} \quad (7)$$

where  $\varepsilon_1$  is the dielectric constant of layer  $A_1$ ,  $d_1$  is the thickness of the same layer,  $N$  is the total number of layers in the multilayer, and  $q$  is the in-plane wave vector. On the other hand, as we discussed in Sec. II, the recursion equation for the KCF multilayer can be expressed as

$$\begin{pmatrix} g_{N+1} \\ h_{N+1} \end{pmatrix} = M_n^{(k)} \begin{pmatrix} g_1 \\ h_1 \end{pmatrix} \equiv \begin{pmatrix} m_{11} & m_{12} \\ m_{21} & m_{22} \end{pmatrix} \begin{pmatrix} g_1 \\ h_1 \end{pmatrix}, \quad (8)$$

where  $m_{11}, m_{12}, m_{21}, m_{22}$  are complicated function relating to the wave vector  $q$ , the frequency  $\varpi$ , the thicknesses  $\{d_i\}$  of layers and the dielectric constants  $\{\varepsilon_i(\varpi)\}$ . By combining Eqs. (7) and (8), we have the dispersion equation as follows:

$$\begin{aligned} (\varepsilon_1^2 - \varepsilon_e^2) e^{2q d_1} m_{11} + (\varepsilon_1 - \varepsilon_e)^2 e^{q d_1} m_{12} - (\varepsilon_1 + \varepsilon_e)^2 e^{q d_1} m_{21} \\ - (\varepsilon_1^2 - \varepsilon_e^2) m_{22} = 0. \end{aligned} \quad (9)$$

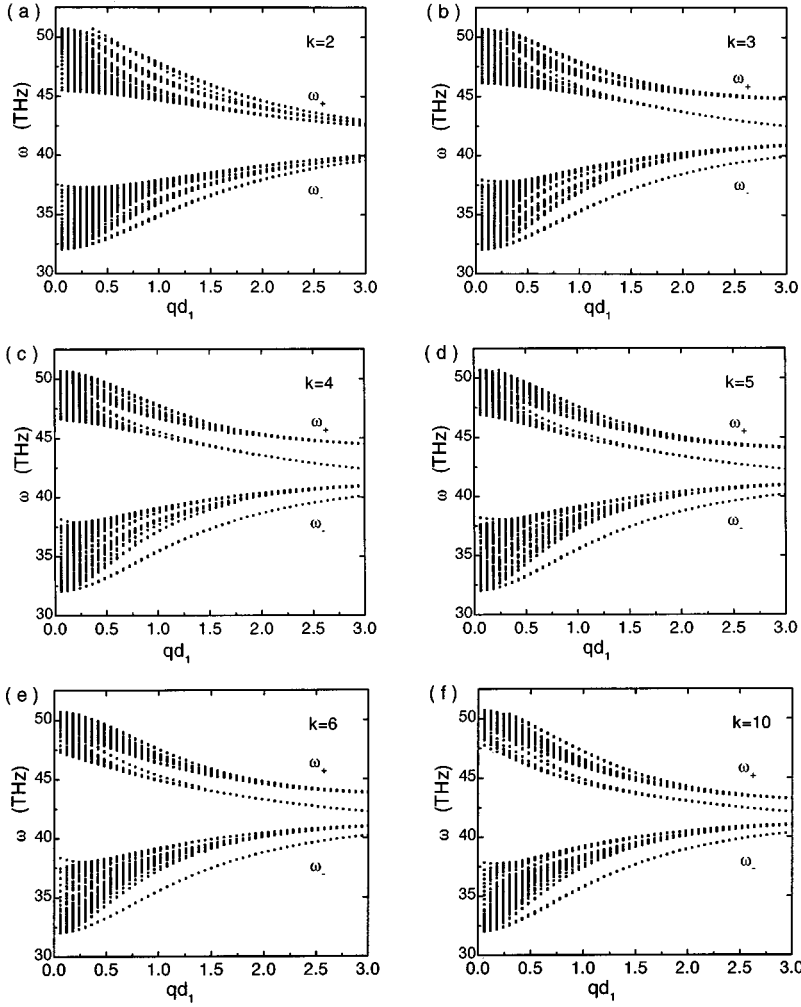


FIG. 1. The dispersion relation of the coupled interface optical phonons for the  $k$ -component Fibonacci dielectric multilayers with the following generation, the total number of layers and the total number of layer  $A_k$ : (a)  $C_{14}^{(2)}$ ,  $N=377$ ,  $N(A_2)=233$ ; (b)  $C_{18}^{(3)}$ ,  $N=872$ , and  $N(A_3)=277$ ; (c)  $C_{21}^{(4)}$ ,  $N=907$ , and  $N(A_4)=250$ ; (d)  $C_{24}^{(5)}$ ,  $N=1001$ , and  $N(A_5)=245$ ; (e)  $C_{24}^{(6)}$ ,  $N=533$ , and  $N(A_6)=119$ ; (f)  $C_{33}^{(10)}$ ,  $N=655$ , and  $N(A_{10})=105$ , respectively.

Obviously, the physical properties of the interface optical phonons of the KCF multilayers are decided by the dispersion equation (9).

Based on Eqs. (6) and (9), the interface optical phonon dispersions in the KCF dielectric multilayers are numerically calculated with free-boundary condition. To demonstrate clearly the effect of the underlying geometrical structures, we consider a simple setting. The dielectric constants  $\{\varepsilon_i(\omega)\}$  corresponding to the  $k$  different layers  $\{A_i\}$  ( $i=1,2,\dots,k-1,k$ ) are chosen as following:  $\{\varepsilon_i\}$  ( $i=1,2,\dots,k-1$ ) are frequency independent, but only the dielectric constant of layer  $A_k$ ,  $\varepsilon_k$ , is frequency dependent. It follows that  $\varepsilon_k(\omega) = \varepsilon_{k,\infty}(\omega^2 - \omega_{k,LO}^2)/(\omega^2 - \omega_{k,TO}^2)$  for alkali halide or polar semiconductor materials, where  $\omega_{k,LO}$  and  $\omega_{k,TO}$  are the longitudinal-optical and transverse-optical frequencies. As an example, we take  $\varepsilon_{k,\infty} = 2.34$ ,  $\omega_{k,TO} = 32.01$  THz, and  $\omega_{k,LO} = 50.74$  THz for NaCl;  $\varepsilon_1 = 3$ ; and  $\varepsilon_i = \varepsilon_1 \times \eta_i$  ( $i=2,3,\dots,k-1$ ), where  $\eta_i$  can be given by Eq. (1). And the environment is supposed to be vacuum, i.e.,  $\varepsilon_e = 1$ . At the same time, the thicknesses of the  $k$  different layers  $\{d_i\}$  are chosen as  $d_i = d_1 \times \eta_i$  ( $i=2,3,\dots,k$ ).

Thereafter the interface optical phonons in the KCF dielectric multilayers with different number of incommensurate intervals  $k$  are investigated. The calculations are performed on different KCF multilayers. Figures 1(a)–1(f) illustrate the dispersion relations of interface optical phonons

for six KCF multilayers with different  $k$ . It is shown that the collective excitations occur only in frequency regimes where the ratio  $\varepsilon_k(\omega)/\varepsilon_i$  ( $i=1,2,\dots,k-1$ ) is negative, because the interface optical phonons may be considered as a linear superposition of surface modes which localized at each interface in the multilayer. In each phonon dispersion spectrum, there exist  $2N_n^{(k)}(A_k) = 2F_{n-k}^{(k)}$  eigenfrequencies, where  $N_n^{(k)}(A_k)$  is the total number of layer  $A_k$  in the multilayer with the generation  $C_n^{(k)}$ , and  $F_{n-k}^{(k)}$  satisfies  $F_j^{(k)} = F_{j-1}^{(k)} + F_{j-k}^{(k)}$  with  $F_i = i+1$  ( $i=0,1,\dots,k-1$ ) (as mentioned in Sec. II). This is due to the fact that the dispersion equation (9) contains  $2N_n^{(k)}(A_k)$  powers of  $\omega$ . It is interesting to note that each spectrum is divided into two dual branches,  $\omega_+$  and  $\omega_-$ . Similar to the situation of periodic multilayers, these two branches are separated by a gap. With the increasing value of  $qd_1$ ,  $\omega_+$  band is down-shifted and  $\omega_-$  band is up-shifted in frequency because of the screening provided by the layers  $\{A_i\}$  ( $i=1,2,\dots,k-1$ ). For high  $qd_1$ , the spectra are highly degenerated. The calculations show that there exist limiting frequencies when the thickness  $d_1$  approaches infinity. For  $k=2$ , as  $d_1 \rightarrow \infty$ , both  $\omega_+$  and  $\omega_-$  bands approach the single-interface surface-mode frequency  $\omega = 41.2772703762$  THz, which satisfies the implicit dispersion relation  $\varepsilon_2(\omega) = -\varepsilon_1$ . When  $k > 2$ , the limiting frequencies obeys the equation  $[\varepsilon_1 + \varepsilon_k(\omega)][\varepsilon_{k-1} + \varepsilon_k(\omega)] = 0$ . For  $k=3$ , the limiting frequencies are  $\omega_+$

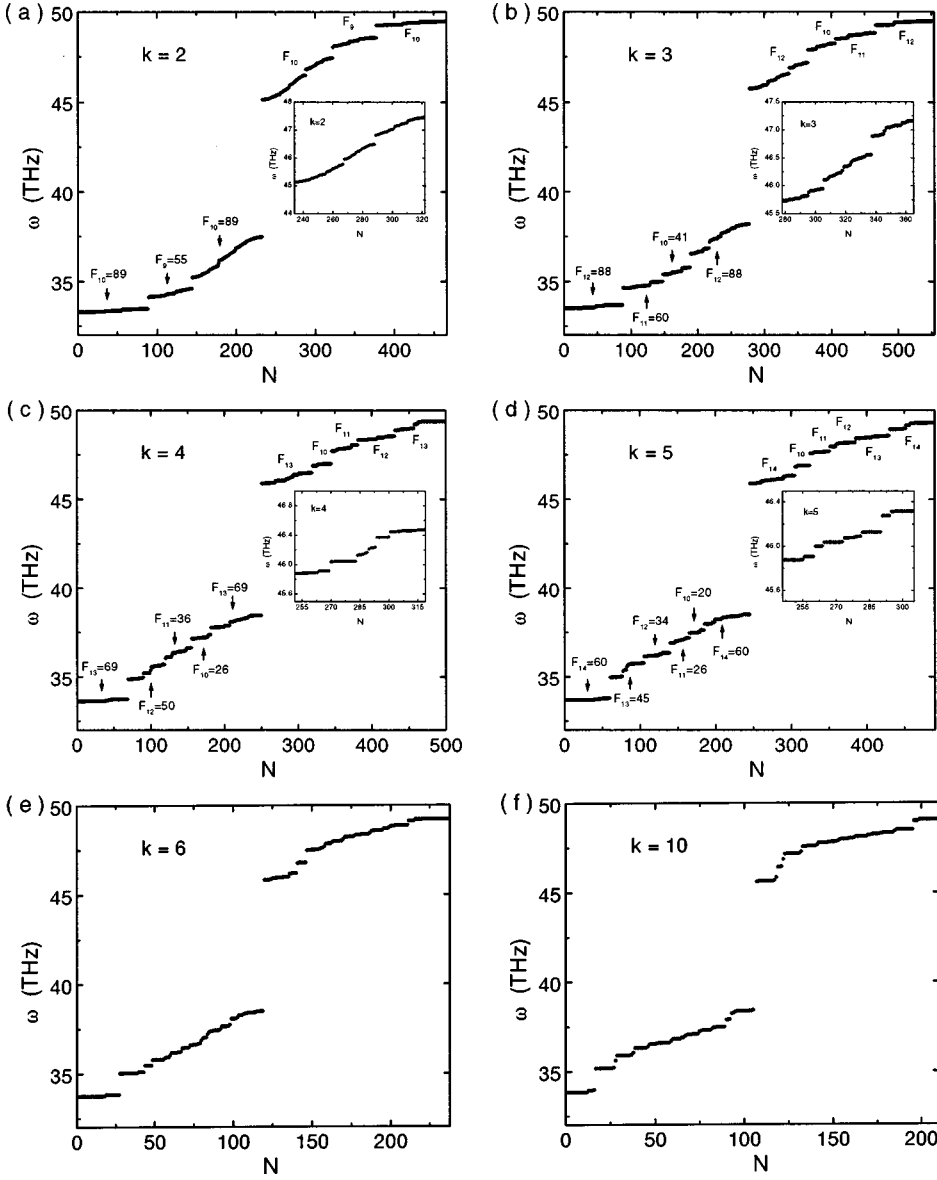


FIG. 2. The eigenfrequency versus number of optical interface modes for the  $k$ -component Fibonacci multilayers for  $qd_1=0.6$ . The insets show the enlarged local regions. The parameters are the same as those in Fig. 1.

$=41.2772703762$  THz and  $\varpi_2=44.6678969765$  THz. For  $k=4$ ,  $\varpi_1$  remains, while  $\varpi_2$  equals  $44.1712652378$  THz. For  $k=5$ ,  $\varpi_1$  keeps the same value, while  $\varpi_2$  reduces to  $43.8206365706$  THz. For  $k=6$  and  $k=10$ ,  $\varpi_2$  decreases further to  $43.5573813549$  THz and  $42.9295309315$  THz, respectively. Actually, these limiting frequencies are the isolated modes, and approach the surface excitations from the isolated slab ( $A_1A_kA_1$ ) and the slab ( $A_1A_kA_{k-1}$ ), respectively, when the thickness  $d_1$  approaches infinity (In this case, it follows that  $d_i \rightarrow \infty$ , where  $i=1, 2, \dots, k$ ).

While for lower  $qd_1$ , the optical phonon dispersion spectra of the KCF multilayers with  $1 < k \leq 5$  consist of  $k+1$  bands. The hierarchical characteristics are clearly shown in Figs. 2(a)–2(d), which gives the eigenfrequency versus the number of interface optical modes in the KCF multilayers with generation  $C_n^{(k)}$  when  $qd_1=0.6$ . We find that the eigenfrequencies in the subbands of  $\varpi_+$  or  $\varpi_-$  are divided into  $k+1$  groups, each group consists of  $F_{n-2k}^{(k)}$ ,  $F_{n-2k-(k-1)}^{(k)}$ ,  $F_{n-2k-(k-2)}^{(k)}$ ,  $\dots$ ,  $F_{n-2k-1}^{(k)}$ , and  $F_{n-2k}^{(k)}$  eigenfrequencies, respectively. So the total number of eigenfrequencies in each band is  $N_n^{(k)}(A_k) \equiv F_{n-k}^{(k)} = F_{n-2k}$

$+ \sum_{i=1}^k F_{n-2k-(k-i)}^{(k)}$ . For example, Fig. 2(b) is for 3-component Fibonacci multilayer with generation  $C_{18}^{(3)}(k=3)$ . The subband  $\varpi_+$  or  $\varpi_-$  has totally  $N_{18}^{(3)}(A_3) \equiv F_{15}^{(3)} = 277$  eigenfrequencies. They are divided into 4 (i.e.,  $k+1$ ) groups, and each group contains  $F_{12}^{(3)} = 88$ ,  $F_{10}^{(3)} = 41$ ,  $F_{11}^{(3)} = 60$ , and  $F_{12}^{(3)} = 88$  eigenfrequencies, respectively. Moreover, every sub-group is separated into  $k+1=4$  groups further as indicated in the inset of Fig. 2(b). In fact, each sub-band in the phonon dispersions of the KCF multilayers with  $1 < k \leq 5$  is self-similar, which consist of  $k+1$  filial generations as illustrated in Figs. 2(a)–2(d) (where  $k$  is the number of different incommensurate intervals). Physically this property originates from the configuration characterizations of the  $k$ -component Fibonacci structures. On the other hand, it is noteworthy that the interface optical phonon dispersion is nonuniform as shown in Figs. 2(a)–2(d). For a specific KCF multilayer, in the  $\varpi_+$  band, the low-frequency region is wider than that in the high-frequency region; while in the  $\varpi_-$  band, the low-frequency region is narrower than that in the high-frequency. This feature reflects the changes of quasiperiodicity in the KCF structures ( $1 < k \leq 5$ ).

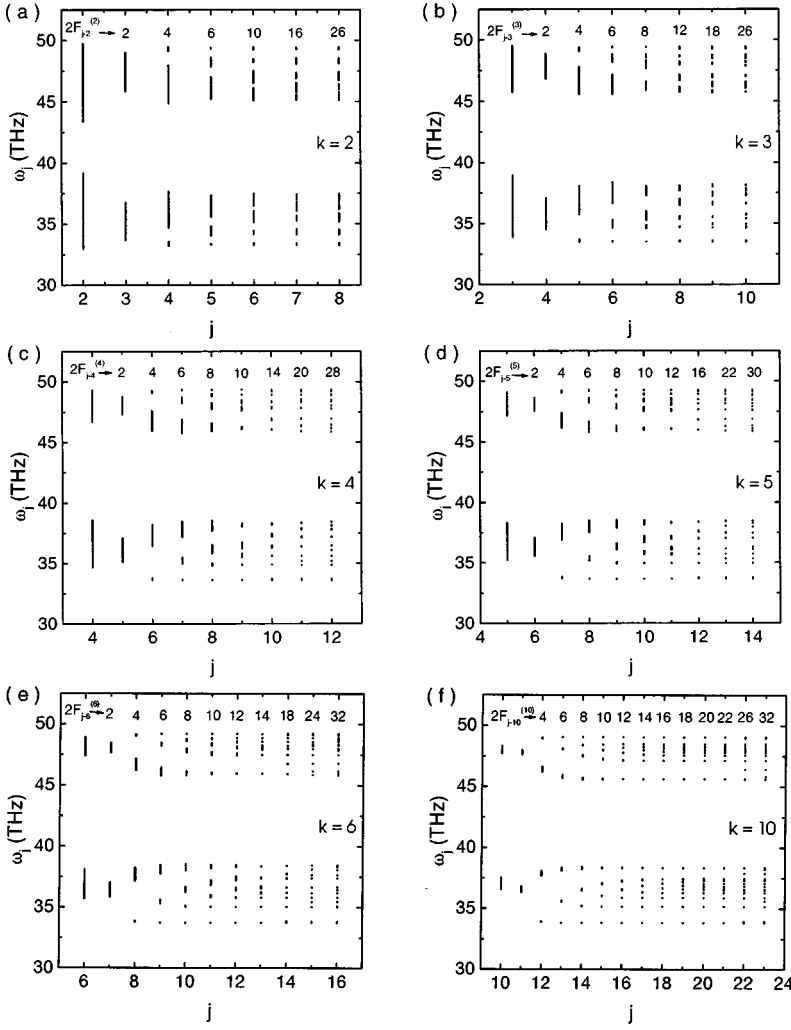


FIG. 3. The frequency spectra of the  $k$ -component Fibonacci multilayers with generation number  $j$ . (a)  $k=2$ ; (b)  $k=3$ ; (c)  $k=4$ ; (d)  $k=5$ ; (e)  $k=6$ ; (f)  $k=10$ .  $\omega_+$  band is up, and  $\omega_-$  band is below.

It is interesting to mention that for lower  $qd_1$ , the optical phonon dispersion spectra of the KCF multilayers with  $k > 5$  do not show self-similarity. Figures 2(e) and 2(f) illustrate the eigenfrequency versus the number of interface optical modes in the KCF multilayers with  $k=6$  and  $k=10$ , respectively. It seems that the eigenfrequencies in the subbands of  $\omega_+$  or  $\omega_-$  are separated into several groups, but the separation rule is not as obvious as that for the case of  $1 < k \leq 5$ . This difference may arise from the fact that the KCF structures with  $k > 5$  do not possess the Posit property and they do not have quasiperiodicity. Further studies on this aspect are being undertaken.

#### IV. FREQUENCY SPECTRA WITH PERIODIC-BOUNDARY CONDITION

The numerical calculations of interface optical phonons in the KCF dielectric multilayers can also be carried out with the periodic-boundary condition, which is usually called rational approximation. The recursion equation for the KCF multilayers can be rewritten as

$$\begin{pmatrix} g_{N+1} \\ h_{N+1} \end{pmatrix} = M_n^{(k)} \begin{pmatrix} g_1 \\ h_1 \end{pmatrix} \equiv \begin{pmatrix} m_{11} & m_{12} \\ m_{21} & m_{22} \end{pmatrix} \begin{pmatrix} g_1 \\ h_1 \end{pmatrix} = e^{iqD} \begin{pmatrix} g_1 \\ h_1 \end{pmatrix}, \quad (10)$$

where  $q$  is the wave vector and  $D$  is the total thickness of the multilayer. We define  $\chi_n^{(k)} = \frac{1}{2} \text{Tr} M_n^{(k)}$ , where  $\text{Tr} M_n^{(k)}$  is the trace of matrix  $M_n^{(k)}$ . Therefore under the rational approximation, the eigenfrequencies satisfy

$$\chi_n^{(k)} = \cos qD. \quad (11)$$

According to Eqs. (6), (10), and (11), the frequency spectra of the KCF dielectric multilayers can be calculated. The parameters, such as the dielectric constants  $\{\varepsilon_i(\omega)\}$  and the thicknesses  $\{d_i\}$  of layers ( $i=1, 2, \dots, k$ ), are the same as described in Sec. III. Figures 3(a)–3(f) illustrates the frequency spectra of the KCF multilayers with  $k$  different incommensurate intervals. It is shown that the frequency spectrum of the KCF multilayer contains two sets of dual structures:  $\omega_+$  and  $\omega_-$ . For the KCF multilayer with an identical  $k$ , by increasing the generation number  $j$ , more and more subbands and gaps emerge. Moreover, the number of subbands in each set  $\omega_+$  or  $\omega_-$  is  $F_{j-k}^{(k)}$ , where  $j$  is the generation number of the KCF multilayer, and  $F_n^{(k)} = F_{n-1}^{(k)} + F_{n-k}^{(k)}$  with  $F_i = i+1$  ( $i=0, 1, \dots, k-1$ ). It is enlightening to compare the interface optical phonon distributions of the KCF multilayers with different  $k$ . As shown in Fig. 3, for the almost identical number of subbands, the widths of subbands decrease when the number of incommensurate intervals  $k$  increases. For example, when  $k=2$  and  $j=8$ , the total width

of  $F_8^{(2)}=26$  subbands is  $\sum_{i=1}^{26}\Delta\varpi_i^{(2)}=3.62851$  THz; when  $k=3$  and  $j=10$ , the total width of  $F_{10}^{(3)}=26$  subbands is  $\sum_{i=1}^{26}\Delta\varpi_i^{(3)}=1.49679$  THz; when  $k=4$  and  $j=12$ , the total width of  $F_{12}^{(4)}=28$  subbands is  $\sum_{i=1}^{28}\Delta\varpi_i^{(4)}=0.586151$  THz; when  $k=5$  and  $j=14$ , the total width of  $F_{14}^{(5)}=30$  subbands is  $\sum_{i=1}^{30}\Delta\varpi_i^{(5)}=0.194019$  THz; when  $k=6$  and  $j=16$ , the total width of  $F_{16}^{(6)}=32$  subbands is  $\sum_{i=1}^{32}\Delta\varpi_i^{(6)}=0.0613213$  THz; and when  $k=10$  and  $j=23$ , the total width of  $F_{23}^{(10)}=32$  subbands is  $\sum_{i=1}^{32}\Delta\varpi_i^{(10)}=0.0229262$  THz. Therefore, the subbands in the frequency spectra of the KCF multilayers gradually develop to be more discrete and much narrower when  $k$  propagates, and the frequency distribution of the KCF multilayers may approach that of a disordered system at a sufficient large  $k$ . From this point of view, when  $k$  varies, the KCF multilayers provide a generic model displaying the evolution from periodicity, quasiperiodicity to randomness. Additionally, Figs. 3(a)–3(f) implies that when the generation number  $j$  is large enough, the frequency spectra of the KCF multilayer are neither discrete nor continuous. These spectra can be characterized by statistical methods such as multifractal analysis.

Multifractal analysis is a tool for characterizing the nature of a positive measure in a statistical sense.<sup>16</sup> Here suppose the measure can be generated by dividing an unit region into pieces  $\{s_i\}$  ( $i=1,2,\dots,N$ ) with measure  $p_i$  and size  $l_i$ . Then the partition function is defined as<sup>14</sup>

$$\Gamma(Q, \tau, \{s_i\}, l) = \sum_{i=1}^N \frac{p_i^Q}{l_i^\tau}, \quad (12)$$

which satisfies

$$\Gamma(Q, \tau) = \lim_{l \rightarrow 0} \Gamma(Q, \tau, \{s_i\}, l) = \text{const.}$$

The parameter  $Q$  provides a ‘‘mathematical microscope’’ for exploring the singular measure in different regions. Once the mass exponent  $\tau(Q)$  is determined, the fractal dimension of the set of pieces with singularity strength  $\alpha, f(\alpha)$ , can be derived from

$$\alpha(Q) = \frac{d\tau(Q)}{dQ},$$

$$f(Q) = Q\alpha(Q) - \tau(Q). \quad (13)$$

The  $f(\alpha)$  singularity spectrum provides a mathematically precise and intuitive description of the nonuniform systems. In our case, we consider the subbands in the frequency spectra  $\varpi_+$  or  $\varpi_-$ ,  $l_i$  represents the width of the  $i$ th subband, and the measure is given as  $p_i = 1/F_{j-k}^{(k)}$ . A straightforward application of multifractal formalism requires the evaluation of exact integral of the frequency measure of the structures with infinite length over small segment of length in the space. Meanwhile the computer time for calculation will increase incredibly. To solve this problem, an approximate scheme is chosen as taking  $\Gamma_{n+1}/\Gamma_n \cong 1$  when the generation number  $n$  is large enough. Figure 4 gives the  $f(\alpha)$  spectra corresponding to the frequency spectra in the KCF multilayers. It is shown that the data points fit into smooth curves, which is a characteristic of an infinite structure. The quantity  $f(\alpha)$  is

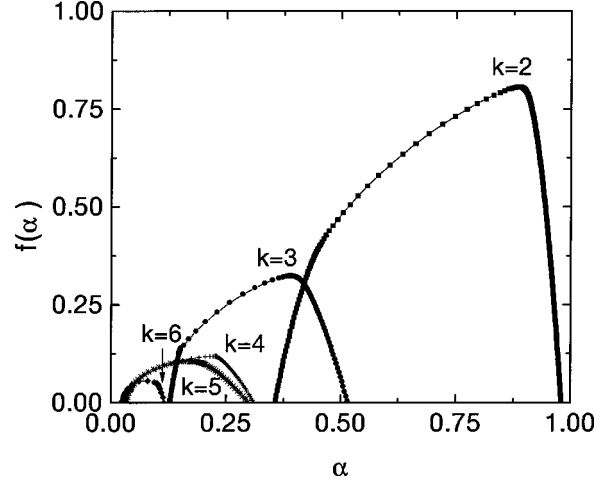


FIG. 4.  $f(\alpha)$  spectra for the frequency distributions of the KCF multilayers where  $k=2$ ,  $\Gamma_{13}/\Gamma_{12}=1$ ;  $k=3$ ,  $\Gamma_{16}/\Gamma_{15}=1$ ;  $k=4$ ,  $\Gamma_{19}/\Gamma_{18}=1$ ;  $k=5$ ,  $\Gamma_{22}/\Gamma_{21}=1$ ;  $k=6$ ,  $\Gamma_{24}/\Gamma_{23}=1$ , respectively.

considered as the dimension of the set of subbands  $\{s_i\}$  in the frequency spectrum. Particularly, it should be emphasized that  $f(\alpha)$  spectrum of a frequency distribution has the following physical implications: (i) The abscissa  $\alpha_0$  of the summit of  $f(\alpha)$  curve, which corresponds to  $Q=0$ , is the strength of a generic singularity. Obviously  $f(\alpha_0) < 1$ , which means that the support of the subbands is not the whole  $\varpi$  axis. Moreover, since the widths of the subbands decrease when  $k$  propagates, the fractal dimension of the support  $f(\alpha_0)$  decreases correspondingly. (ii) The extremes  $\alpha_{\min}$  and  $\alpha_{\max}$  of the abscissa of a  $f(\alpha)$  curve represent the minimum and the maximum of the singularity exponent  $\alpha$  which acts as an appropriate weight in frequency measure. In fact,  $\alpha_{\min}$  and  $\alpha_{\max}$  characterize the scaling properties of the most concentrated and most rarefied region of the frequency measure respectively. As the increasing of the number of incommensurate intervals  $k$  in the KCF multilayers,  $\Delta\alpha = \alpha_{\max} - \alpha_{\min}$  decreases gradually. This may imply that the frequency distribution of the KCF multilayer approaches the behavior of a random system when  $k$  increases. The above scaling analysis indicates the frequency spectrum of the KCF multilayers is a generic multifractal. When  $k$  increases, the narrower subbands and wider gaps are found in the frequency spectra of the KCF multilayers, the fractal dimensions definitely decrease.

## V. CONCLUSION

We have presented the interface optical phonons in the  $k$ -component Fibonacci (KCF) dielectric multilayers, which contains  $k$  different incommensurate intervals and can be generated by the deterministic substituted rules. Although the KCF structures have long-range order, they are highly aperiodic. For studying the physical properties related to them, we are not able to find a powerful scheme equivalent to Bloch theorem for periodic structures. What we can do is to use finite structures to approach the infinity. Meanwhile, the transfer-matrix method is helpful to obtain the dispersion relations and frequency spectra of the collective excitations, and boundary conditions should be introduced. Both free-boundary condition and periodic-boundary condition are

commonly used. With the free-boundary condition, the interface optical phonon dispersion in the KCF multilayers forms discrete spectra and shows hierarchical characteristic. Particularly for the KCF multilayers with  $1 < k \leq 5$ , which is quasiperiodic, the phonon dispersion spectra possesses two dual self-similar structures with  $k+1$  filial generations (where  $k$  is the number of different incommensurate intervals). With the periodic-boundary condition, the frequencies of interface optical phonons in the KCF multilayers are punctuated continuous, and it is expected to display a multifractal behavior. Multifractal analysis reveals that the dimension spectrum of singularities  $f(\alpha)$  is a smooth function with a summit  $f(\alpha_0) < 1$ . The frequencies do not have an absolutely continuous component. Therefore, the frequency distributions of the interface optical phonons in the KCF multilayers are singular continuous and possess multifractal properties. Evidently there are some differences on the interfacial optical phonon spectra of the KCF dielectric multilayers corresponding to the periodic and free-boundary conditions. We expect that such a difference originates from the variation of the degrees of freedom in the systems. With the free-boundary condition, the number of the degrees of free-

dom in the KCF dielectric multilayer system is limited, therefore the phonon dispersion displays the pointlike discrete spectra. While with the periodic-boundary condition, the “multilayer” is regarded as an “unit” and repeated periodically. So the number of the degrees of freedom in the system increases significantly. As a result, the phonon frequency distributions of the KCF dielectric multilayers are punctuated continuously. Generally the results from the periodic-boundary condition have some advantages in scaling analysis, while the results from the free-boundary condition may be easier to compare with experiments. We expect that Raman scattering investigations on the interface optical phonons in the KCF dielectric multilayers will provide interesting information in a further study.

#### ACKNOWLEDGMENTS

This work was supported by the National Natural Science Foundation of China, the State Science and Technology Commission of China, and the provincial Natural Science Foundation of Jiangsu.

- 
- <sup>1</sup>R. E. Camley, T. S. Rahman, and D. L. Mills, Phys. Rev. B **27**, 261 (1983); M. Grimsditch, M. R. Khan, A. Kueny, and I. K. Schuller, Phys. Rev. Lett. **51**, 498 (1983); P. Grünberg and K. Mika, Phys. Rev. B **27**, 2955 (1983).
- <sup>2</sup>R. E. Camley and D. L. Mills, Phys. Rev. B **29**, 1695 (1984); G. F. Giuliani and J. J. Quinn, Phys. Rev. Lett. **51**, 919 (1983); D. Olego, A. Pinczuk, A. C. Gossard, and W. Wiegmann, Phys. Rev. B **25**, 7867 (1982); B. L. Johnson, J. T. Weiler, and R. E. Camley, *ibid.* **32**, 6544 (1985); B. L. Johnson and R. E. Camley, *ibid.* **38**, 3311 (1988).
- <sup>3</sup>A. Kueny and M. Grimsditch, Phys. Rev. B **26**, 4699 (1982); R. E. Camley, B. Djafari-Rouhani, L. Dobrzynski, and A. A. Maradudin, *ibid.* **27**, 7318 (1983); C. Colvard, T. A. Gant, M. V. Klein, R. Merlin, R. Fischer, H. Morkoc, and A. C. Gossard, *ibid.* **31**, 2080 (1985); A. K. Sood, J. Menéndez, M. Cardona, and K. Ploog, Phys. Rev. Lett. **54**, 2115 (1985); E. P. Pokatilov and S. I. Beril, Phys. Status Solidi B **110**, K75 (1982); Kun Huang and Bangfen Zhu, Phys. Rev. B **38**, 13 377 (1988).
- <sup>4</sup>G. J. Jin, S. S. Kang, Z. D. Wang, A. Hu, and S. S. Jiang, Phys. Rev. B **54**, 11 883 (1996).
- <sup>5</sup>Nian-hua Liu, Yi He, Wei-guo Feng, and Xiang Wu, Phys. Rev. B **52**, 11 105 (1995).
- <sup>6</sup>R. Merlin, K. Bajema, R. Clarke, F.-Y. Juang, and P. K. Bhattacharya, Phys. Rev. Lett. **55**, 1768 (1985).
- <sup>7</sup>M. Kohmoto, B. Sutherland, and C. Tang, Phys. Rev. B **35**, 1020 (1987).
- <sup>8</sup>J. Todd, R. Merlin, R. Clarke, K. M. Mohanty, and J. D. Axe, Phys. Rev. Lett. **57**, 1157 (1986); A. Hu, C. Tien, X. Li, Y. Wang, and D. Feng, Phys. Lett. A **119**, 313 (1986).
- <sup>9</sup>K. Bajema and R. Merlin, Phys. Rev. B **36**, 4555 (1987); C. Wang and R. A. Barrio, Phys. Rev. Lett. **61**, 191 (1988).
- <sup>10</sup>J.-P. Desideri, L. Macon, and D. Sornette, Phys. Rev. Lett. **63**, 390 (1989); K. Kono, S. Nakada, Y. Narahara, and Y. Ootuka, J. Phys. Soc. Jpn. **60**, 368 (1991).
- <sup>11</sup>G. J. Jin, Z. D. Wang, A. Hu, and S. S. Jiang, J. Phys.: Condens. Matter **8**, 10 285 (1996).
- <sup>12</sup>A. Hu, Z. X. Wen, S. S. Jiang, W. T. Tong, R. W. Peng, and D. Feng, Phys. Rev. B **48**, 829 (1993).
- <sup>13</sup>R. W. Peng, A. Hu, S. S. Jiang, C. S. Zhang, and Duan Feng, Phys. Rev. B **46**, 7816 (1992); R. W. Peng, Mu Wang, A. Hu, S. S. Jiang, J. G. Jin, and D. Feng, *ibid.* **52**, 13 310 (1995); P. Tong, *ibid.* **52**, 16 301 (1995); M. K. Ali and G. Gumbs, *ibid.* **38**, 7091 (1988); Y. Liu, H. Han, B. Cheng, and C. Luan, *ibid.* **43**, 13 240 (1991); M. Cai, Y. Liu, and W. Deng, *ibid.* **49**, 5429 (1994).
- <sup>14</sup>T. C. Halsey, M. H. Jensen, L. P. Kadanoff, I. Procaccia, and B. I. Shraiman, Phys. Rev. A **33**, 1141 (1986).
- <sup>15</sup>P. Meakin, A. Coniglio, H. E. Stanley, and T. A. Witten, Phys. Rev. A **34**, 3325 (1986).
- <sup>16</sup>G. Paladin and A. Vulpiani, Phys. Rep. **156**, 147 (1987); J. Feder, *Fractal* (Plenum, New York, 1988); Ashvin Chhabra and Roderick V. Jensen, Phys. Rev. Lett. **62**, 1327 (1989); C. Godrèche and J. M. Luck, J. Phys. A **23**, 3769 (1990).